Backbone-Ion Engineering Enables MOF-Derived Single Platinum Atomic Arrays for High-Performance Photovoltaic Devices

Jingwen He[1], Fei Song[3], Weiwei Zhang[1,2], Wenjun Wu[1*]

[1] Shanghai Key Laboratory of Functional Materials Chemistry, Key Laboratory for Advanced Materials and Joint International Research Laboratory of Precision Chemistry and Molecular Engineering, Feringa Nobel Prize Scientist Joint Research Center, Institute of Fine Chemicals, Frontiers Science Center for Materiobiology and Dynamic Chemistry, School of Chemistry and Molecular Engineering, East China University of Science and Technology, Shanghai, 200237, P. R. China.

[2] Center of Photosensitive Chemicals Engineering, East China University of Science and Technology, Shanghai, 200237, P. R. China

[3] Shanghai Synchrotron Radiation Faciality, Shanghai Advanced Research Institute, Chinese Academy of Sciences, Shanghai, China

*E-Mail: wjwu@ecust.edu.cn

MATERIALS AND METHODS

Materials

Copper nitrate trihydrate ($Cu(NO_3)_2 \cdot 3H_2O$, 99%), nickel nitrate hexahydrate ($Ni(NO_3)_2 \cdot 6H_2O$, 99%), cobalt nitrate hexahydrate ($Co(NO_3)_2 \cdot 6H_2O$, 99%), polyvinylpyrrolidone (PVP, average Mn = 58,000), benzonitrile (99%), N, N-dimethylformamide (DMF, 99.8%), pyrrole (98%), 4-formylbenzoic acid (99%), propionic acid (99%), platinum dichloride ($PtCl_2$, 98%), potassium tetrachloroplatinate(II) (K_2PtCl_4, 98%), and trifluoroacetic acid (CF_3COOH, 99%) were purchased from Adamas. Deionized water was obtained from a Milli-Q purification system. All chemicals were used as received without further purification.

Catalyst Preparation

Synthesis of meso-tetracarboxyphenyl porphyrin (TCPP).

10 mL of pyrrole (98%, light brown solution) was distilled under vacuum at 80°C to give 5 mL of a clear solution. 4-formylbenzoic acid (3.0 g, 20 mmol) was dissolved in propionic acid (100 mL) and freshly distilled pyrrole (1.4 mL, 20 mmol) was added by syringe. The solution immediately darkened and was refluxed for 15 hours. The mixture was chilled in a fridge for 10 hours before collection of the solid by vacuum filtration. The solid was washed with hot water (2 x 20 mL) and dried under vacuum to give the product as a black powder (3.23 g, 4.0 mmol, 80 %). ^{1}H NMR (400 MHz, DMSO-d6): δ 13.31 (s, 4H), 8.86 (s, 8H), 8.40-8.34 (q, 16H), -2.94 (s, 2H).

Synthesis of Platinum(II) tetrakis(4-carboxyphenyl)porphyrin Complex (Pt-TCPP).

$PtCl_2$ (60 mg, 0.225 mmol) and TCPP (59.5 mg, 0.0753 mmol) were added to a dry round bottomed 25 mL flask with anhydrous benzonitrile and degassed with a stream of N_2 for 20 min. The solution was stirred and refluxed under N_2, and then the solvent was removed under vacuum. The crude product was purified with column chromatography on silica gel with CH_2Cl_2 and hexane as the eluent. Recrystallization from CH_2Cl_2 / hexane gave Pt(II) porphyrin complex as crystals (40% yield). ^{1}H NMR (400 MHz, DMSO-d6): δ 8.76 (s, 8H), 8.37-8.26 (q, 16H).

Synthesis of Pt single atoms coordinated 2D-MOFs (Cu@Pt-SACs)

Typically, $Cu(NO_3)_2 \cdot 3H_2O$ (5 mg), trifluoroacetic acid (50 μL) and PVP (20.0 mg) were dissolved in a mixture of DMF (12 mL) and ethanol (3 mL) in a 30 mL vial. Pt-TCPP (10 mg) was dissolved

in a mixture of DMF (4 mL) and then ethanol (1 mL) was added drop wisely into the aforementioned solution under stirring. After that, the mixed solution in the capped vial was sonicated for 15 min, and then the capped vial was heated at 80 ºC for 12 h. The resulting nanosheets were washed twice with ethanol, and then collected by centrifuge at 4000 r.p.m for 10 min. Finally, the obtained Cu@Pt-SACs were then dried in vacuum overnight.

Synthesis of Pt single atoms coordinated 2D-MOFs (Ni@Pt-SACs)

Typically, $Ni(NO_3)_2 \cdot 6H_2O$ (5 mg), trifluoroacetic acid (50 μL) and PVP (20.0 mg) were dissolved in a mixture of DMF (12 mL) and ethanol (3 mL) in a 30 mL vial. Pt-TCPP (10 mg) was dissolved in a mixture of DMF (4 mL) and then ethanol (1 mL) was added drop wisely into the aforementioned solution under stirring. After that, the mixed solution in the capped vial was sonicated for 15 min, and then the capped vial was heated at 100 ºC for 4 h. The resulting nanosheets were washed twice with ethanol, and then collected by centrifuge at 4000 r.p.m for 10 min. Finally, the obtained Ni@Pt-SACs were then dried in vacuum overnight.

Synthesis of Pt single atoms coordinated 2D-MOFs (Co@Pt-SACs)

Co@Pt-SACs were synthesized via a hydrothermal method. Briefly, $Co(NO_3)_2 \cdot 6H_2O$ (5 mg), trifluoroacetic acid (50 μL), and PVP (20 mg) were dissolved in a mixed solvent of DMF (12 mL) and ethanol (3 mL) in a 30 mL vial. Pt-TCPP (10 mg) was first dissolved in DMF (4 mL), and ethanol (1 mL) was subsequently added dropwise under stirring. The two solutions were then combined, sonicated for 15 min in a sealed vial, and heated at 120 °C for 4 h. The resulting product was washed twice with ethanol, collected by centrifugation at 4000 r.p.m. for 10 min, and dried under vacuum overnight. Cu@Pt-SACs and Ni@Pt-SACs were prepared following the same procedure as described above for Co@Pt-SACs, except that the reaction temperature was adjusted accordingly. Detailed synthetic procedures are provided in the Supporting Information.

Synthesis of 2D-MOFs without Pt (Cu@MOFs)

The synthesis method for Co@MOFs is similar to the synthesis method described above. $Cu(NO_3)_2 \cdot 3H_2O$ (5 mg), trifluoroacetic acid (50 μL) and PVP (20.0 mg) were dissolved in a mixture of DMF (12 mL) and ethanol (3 mL) in a 20 mL vial. Then, the TCPP (10 mg) dissolved in a mixture of DMF (4 mL) and ethanol (1 mL) was added drop wisely into the aforementioned solution

under stirring. After that, the mixed solution in the capped vial was sonicated for 15 min, and then the capped vial was heated at 80 ºC for 4 h. The resulting nanosheets were washed twice with ethanol, and then collected by centrifuge at 4000 r.p.m for 15 min. Finally, the obtained Cu@MOFs were then dried in vacuum overnight.

Synthesis of 2D-MOFs without Pt (Ni@MOFs)

The synthesis method for Ni@MOFs is similar to the synthesis method described above. $Ni(NO_3)_2 \cdot 6H_2O$ (5 mg), trifluoroacetic acid (50 μL) and PVP (20.0 mg) were dissolved in a mixture of DMF (12 mL) and ethanol (3 mL) in a 20 mL vial. Then, the TCPP (10 mg) dissolved in a mixture of DMF (4 mL) and ethanol (1 mL) was added drop wisely into the aforementioned solution under stirring. After that, the mixed solution in the capped vial was sonicated for 15 min, and then the capped vial was heated at 100 ºC for 4 h. The resulting nanosheets were washed twice with ethanol, and then collected by centrifuge at 4000 r.p.m for 15 min. Finally, the obtained Ni@MOFs were then dried in vacuum overnight.

Synthesis of 2D-MOFs without Pt (Co@MOFs)

The synthesis of Co@MOFs followed a procedure similar to that described above. Typically, $Co(NO_3)_2 \cdot 6H_2O$ (5 mg), trifluoroacetic acid (50 μL), and PVP (20 mg) were dissolved in a mixed solvent of DMF (12 mL) and ethanol (3 mL) in a 20 mL vial. Separately, TCPP (10 mg) was dissolved in DMF (4 mL), and ethanol (1 mL) was added dropwise under stirring. The resulting solution was then introduced into the former mixture, sonicated for 15 min in a sealed vial, and heated at 120 °C for 4 h. The obtained product was washed twice with ethanol, collected by centrifugation at 4000 r.p.m. for 15 min, and dried under vacuum overnight. Cu@MOFs and Ni@MOFs were prepared using the same protocol as Co@MOFs, except that the reaction temperature was adjusted. Detailed procedures are provided in the Supporting Information.

Charactrization

Catalyst characterization

Transmission electron microscopy (TEM) images and elemental mapping of the catalysts were obtained on a Talos F200X transmission electron microscope. Atomic-resolution high-angle annular dark-field scanning transmission electron microscopy (AC-HAADF-STEM) images were recorded using a Themis Z instrument. X-ray photoelectron spectroscopy (XPS) was performed on a Thermo Scientific K-Alpha spectrometer. Powder X-ray diffraction (PXRD) was recorded on a

Bruker D8 Advance X-ray powder diffractometer. Nuclear magnetic resonance (NMR) spectra were collected on a Bruker Avance Neo 400WB superconducting NMR spectrometer. The specific surface area was determined by the Brunauer–Emmett–Teller (BET) method using a Micromeritics ASAP 2460 analyzer. Elemental analysis was conducted with an Agilent 5800 inductively coupled plasma optical emission spectrometer (ICP-OES). X-ray absorption fine structure (XAFS) spectra were acquired at the BL20U beamline of the Shanghai Synchrotron Radiation Facility (SSRF) and analyzed using Athena and Artemis software (version 0.9.26). Grazing-incidence wide-angle X-ray scattering (GIWAXS) measurements were carried out at the BL14B1 beamline of SSRF, with data analysis performed using FIT2D software (version beta 18_002).

Device Characterization

The photocurrent density–voltage (J–V) characteristics were measured using a Keithley 2400 sourcemeter under simulated air mass 1.5 (AM1.5) illumination (100 mW cm^{-2}) provided by an Oriel 91106 solar simulator (Newport, USA), with a scan rate of 20 mV s^{-1}. The device active area was approximately 0.25 cm^2, and a mask with an oblong aperture (0.0875 cm^2) was applied during J–V measurements. Incident photon-to-current conversion efficiency (IPCE) spectra were recorded using a Newport-74125 system (Newport Instruments). Electrochemical impedance spectroscopy (EIS) was performed on a ZAHNER ENNIUM electrochemical workstation over a frequency range from 1 Hz to 3.92 MHz.

Theoretical calculations

Performed using the Gaussian 16 Revision A.03 software package, optimized the molecular structures of the three Pt@SACs with the em=gd3bj pbe1pbe density functional theory (DFT) method. Among them, the basis set 6-311G(d) was chosen for the calculation of C, H, O and N atom. And the basis set Lanl2dz was chosen for the calculation of Pt, Cu, Ni and Co atom.

Preparation of Device

Pt electrode: Some isopropanol solution of chloroplatinic acid (0.02 M) were added dropwise to the cleaned FTO conductive glass by spin coating (2000 rmp), and a thin film of Pt was formed after calcining at 400 °C for 15 min.

Pt@SACs electrode: The ethanol colloid of Pt@SACs was spin-coated (3000 rpm) onto the surface of the Pt electrode, and nitrogen was introduced into the tube furnace. The electrode was

then sintered at 300℃ for 15 minutes to obtain the Pt@SACs electrode.

Preparation of liquid electrolyte: 0.5 M tetra-butylpyridine (TBP), 0.05M iodine, 0.1 M lithium iodide, 0.1 M 1,3-dimethyl-3-propylimidazolium iodide (DMPII), 0.6M 1-butyl-3-methylimidazolium iodide (BMII), 0.1 M guanidinium thiocyanate (GuSCN) were dissolved in a mixture of acetonitrile and valeronitrile (85: 15, V: V).

Preparation of TiO_2 photoanode: Titanium dioxide paste 18NR-T and 18NR-AO were deposited onto clean FTO conductive glass by screen printing, respectively. The TiO_2 electrodes (area = 0.25 cm^2) were gradually heated in muffle furnace with programmed temperature at 325 °C for 5 min, 375 °C for 5 min, 450 °C for 15 min and 500 °C for 15 min, cooled to room temperature, treated with a dilute solution of $TiCl_4$ (40 mM, 75 °C for 30 min) and sintered at 500 °C for 30 min. The electrodes were allowed to cool (80-100 °C) and immersed into an ethanol solution of N719 (3 mM) overnight.

Device Characterization. The photocurrent density-voltage characteristics were measured by a Keithley 2400 sourcemeter under air mass 1.5 (AM1.5) illumination at 100 mW cm^{-2} using an Oriel 91106 solar simulator (Newport, USA) with a scan rate of 20 mV s^{-1}. The active area of the device is approximately 0.25 cm^2, and a mask with an oblong aperture (0.0875 cm^2) was applied under J-V tests. The IPCE spectra were recorded by Newport-74125 system (Newport Instruments). Electrochemical impedance spectroscopy (EIS) was measured on ZAHNER ENNIUM electrochemical workstations in the frequency range from 1 Hz to 3.92 MHz.

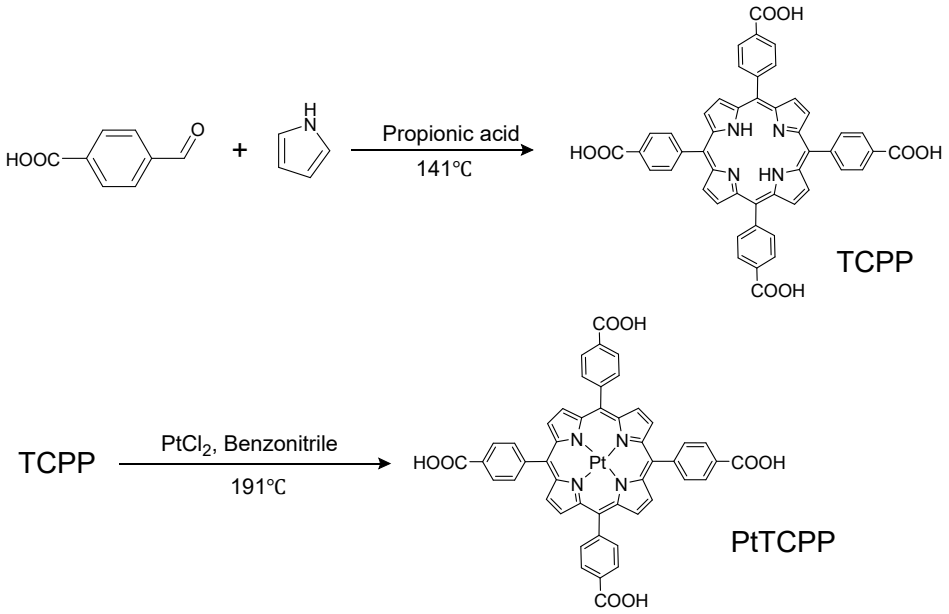

Figure S1. Schematic diagram of the synthesis of TCPP and PtTCPP.

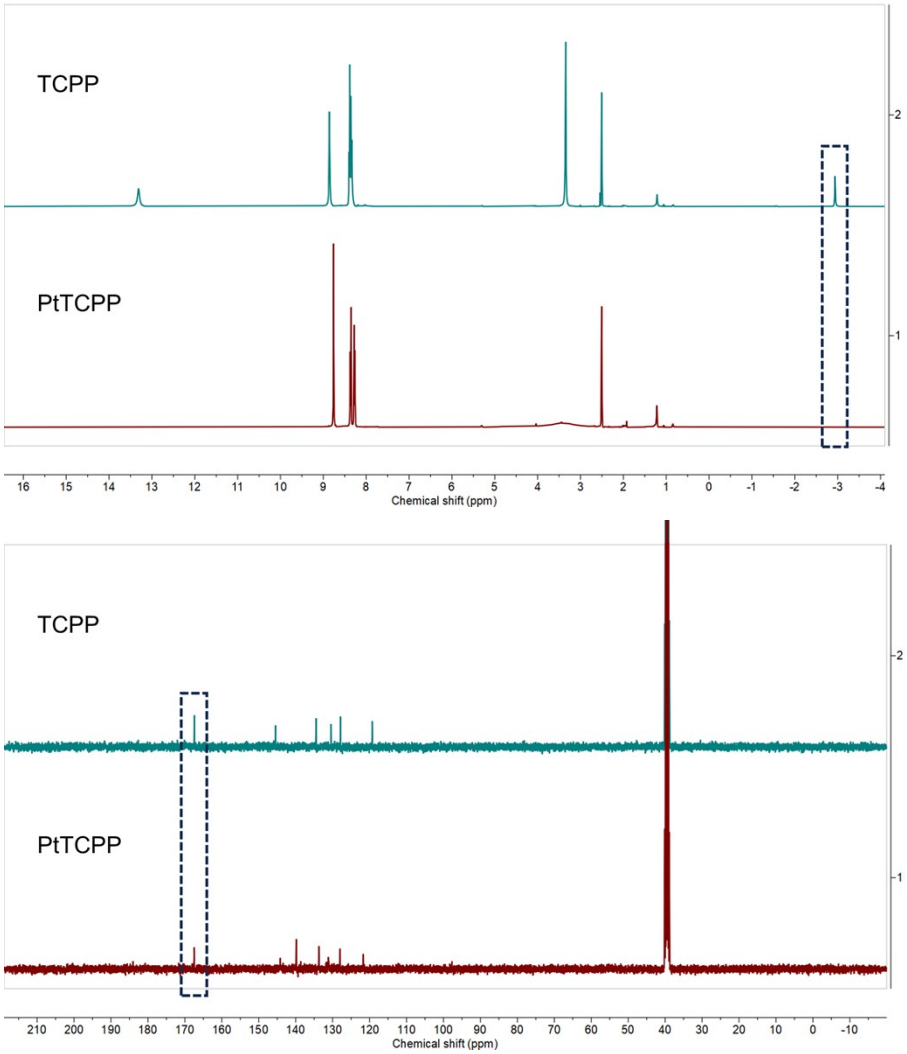

Figure S2. The ^{1}H NMR and ^{1}C NMR spectra of TCPP and PtTCPP are shown in Figure S2. The 1H NMR spectrum of TCPP exhibits a peak at -2.94 ppm, which is attributed to the proton in the free –NH group, whereas this peak is absent in the spectrum of PtTCPP. This indicates the presence of Pt-N coordination. However, the carboxyl peak (13.31 ppm) is absent in PtTCPP. The active hydrogen rapidly exchanges with the deuterium atoms of the deuterated reagent, resulting in no peak appearing in the NMR spectrum. However, in the ^{1}C NMR spectrum, a characteristic peak for the carboxyl carbon appears at 165 ppm in both TCPP and PtTCPP, indicating that the carboxyl group in PtTCPP was not lost during synthesis.

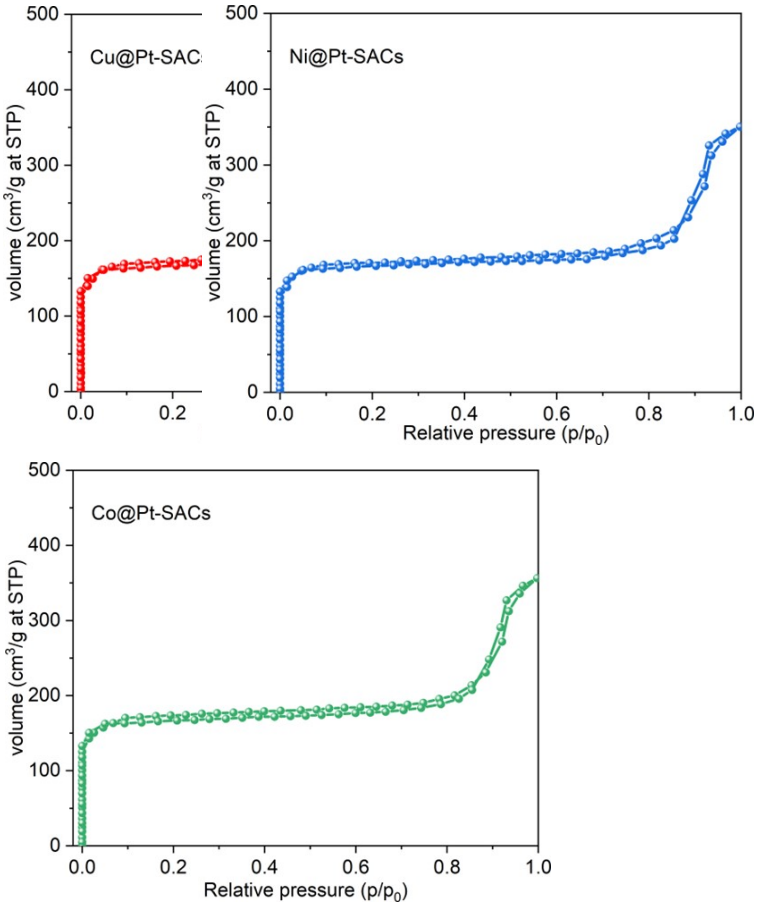

Figure S3. Nitrogen adsorption/ desorption isotherm of Cu@Pt-SACs, Ni@Pt-SACs and Co@Pt-SACs. The BET surface of Cu@Pt-SACs, Ni@Pt-SACs and Co@Pt-SACs is calculated as 551.3 m^2 g^{-1}, 549.8 m^2 g^{-1} and 552.7 m^2 g^{-1}, respectively.

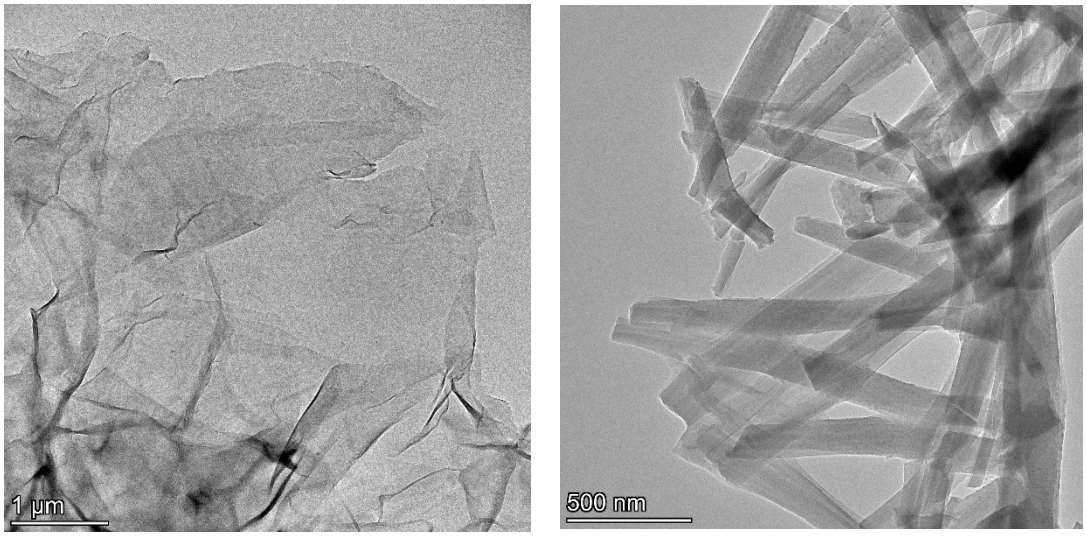

Figure S4. TEM image of Cu@Pt-SACs (left) and Ni@Pt-SACs (right).

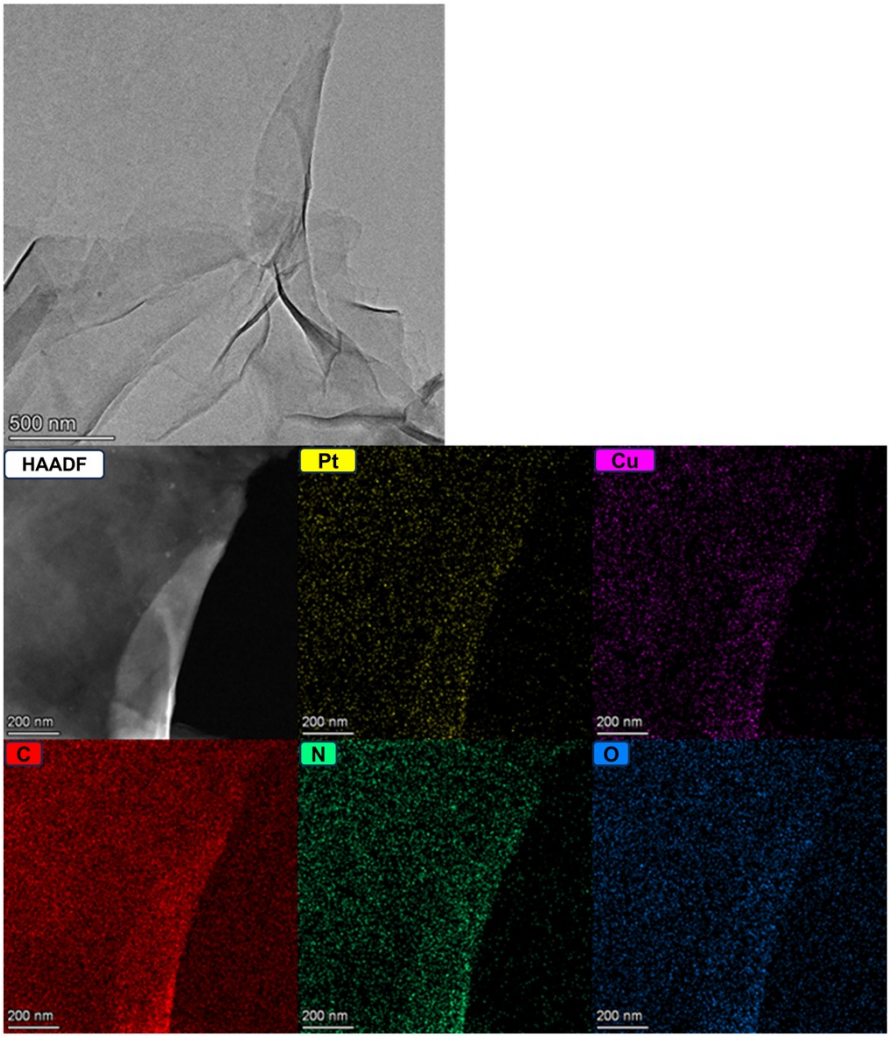

Figure S5. Elemental mapping spectra of Cu@Pt-SACs.

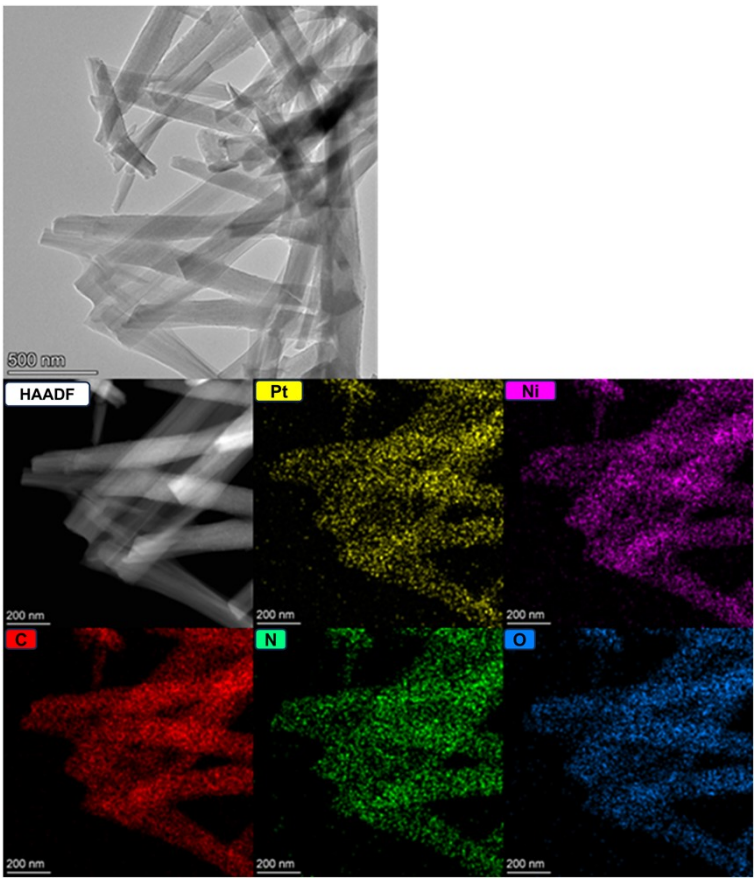

Figure S6. Elemental mapping spectra of Ni@Pt-SACs.

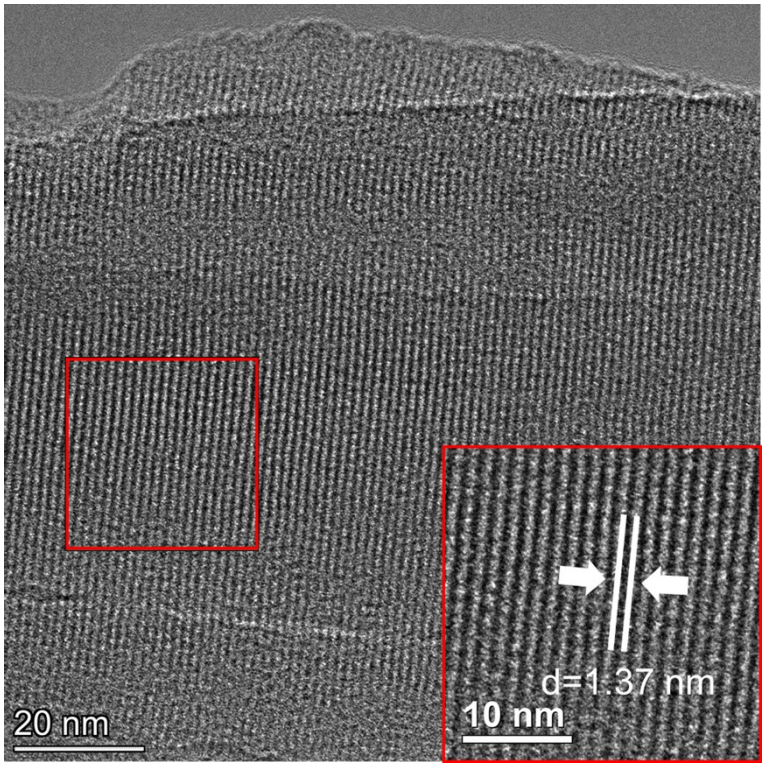

Figure S7. HRTEM image of Cu@Pt-SACs, which shows the lattice spacing of 1.37 nm.

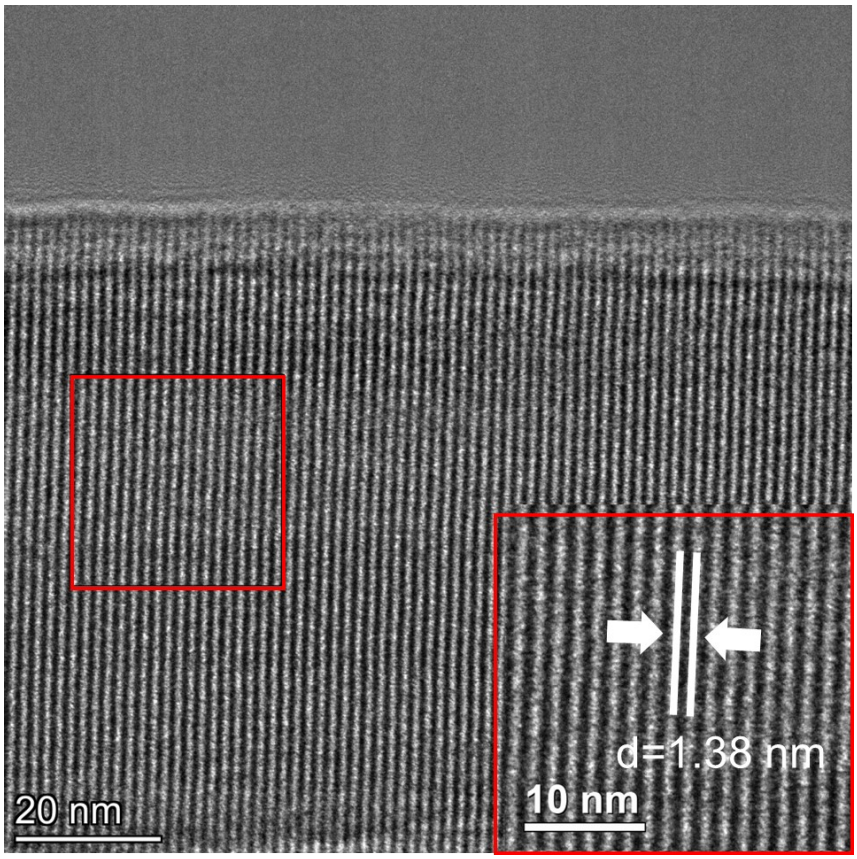

Figure S8. HRTEM image of Ni@Pt-SACs, which shows the lattice spacing of 1.38 nm.

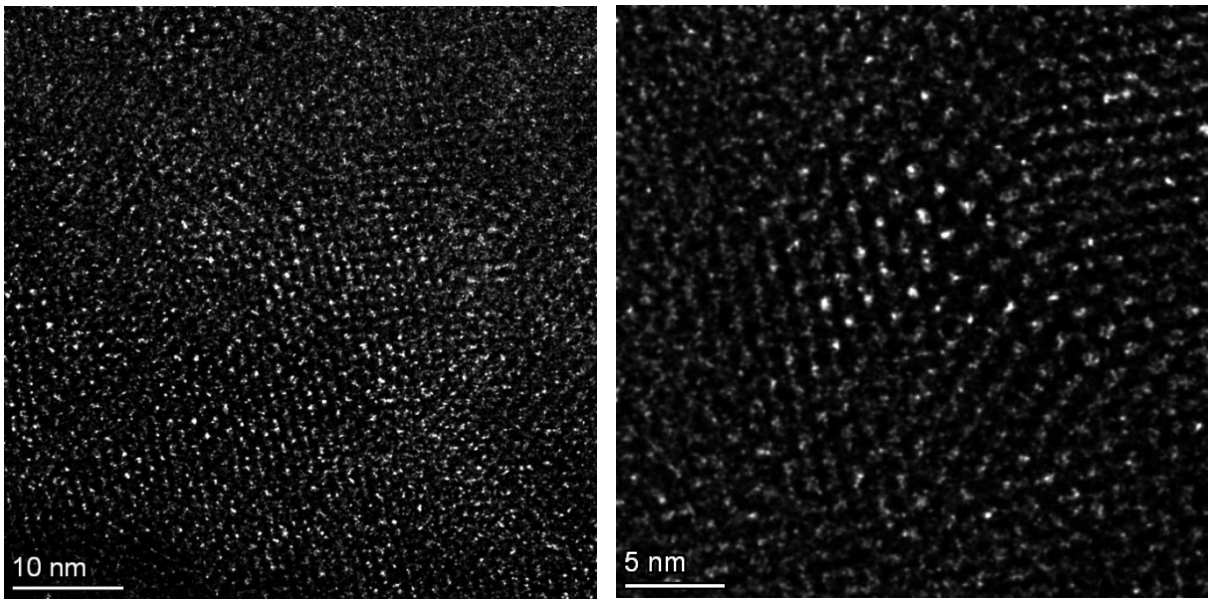

Figure S9.AC-HAADF-STEM image of the Cu@Pt-SACs (left) and Ni@Pt-SACs (right).

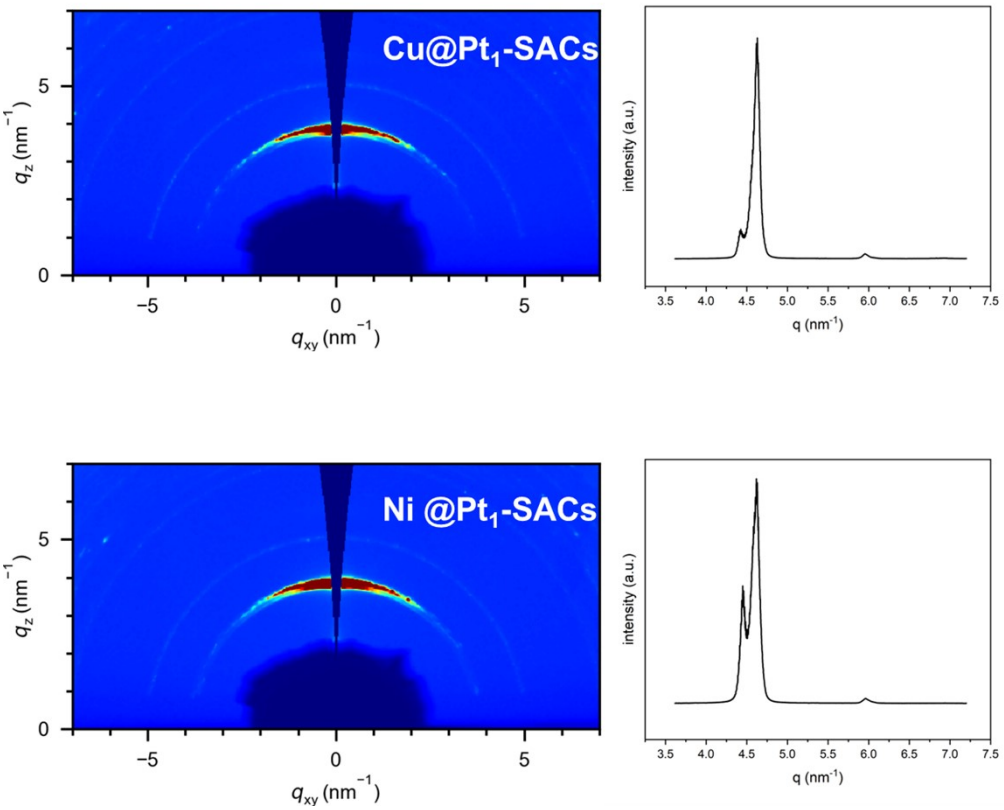

Figure S10. GIWAXS of the Cu@Pt-SACs (up) and Ni@Pt-SACs (down). Integral results are 1.37nm and 1.37nm.

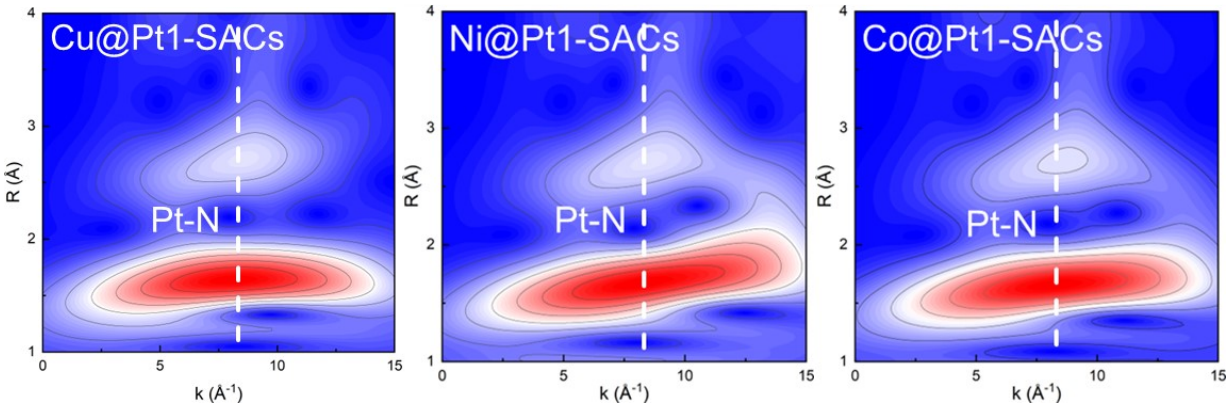

Figure S11. WT-EXAFS spectra of Cu@Pt-SACs, Ni@Pt-SACs, Co@Pt-SACs.

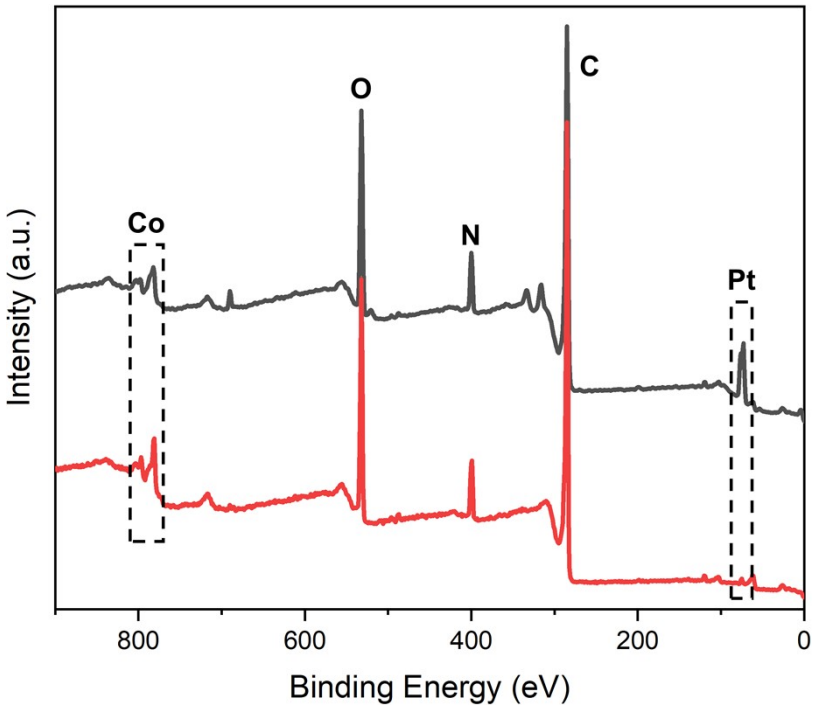

Figure S12. XPS survey spectra of Co@MOFs and Co@Pt-SACs.

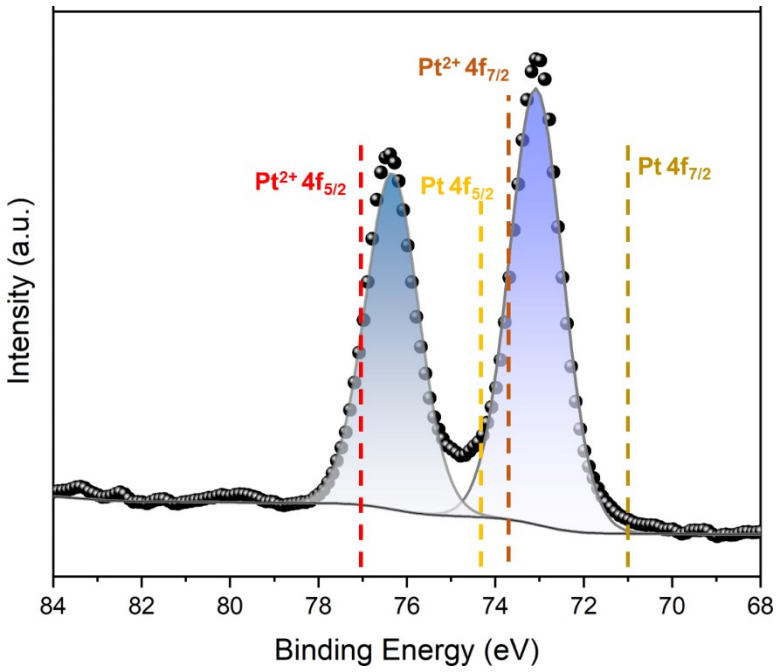

Figure S13. High-resolution Pt 4f XPS spectra of Co@Pt-SACs.

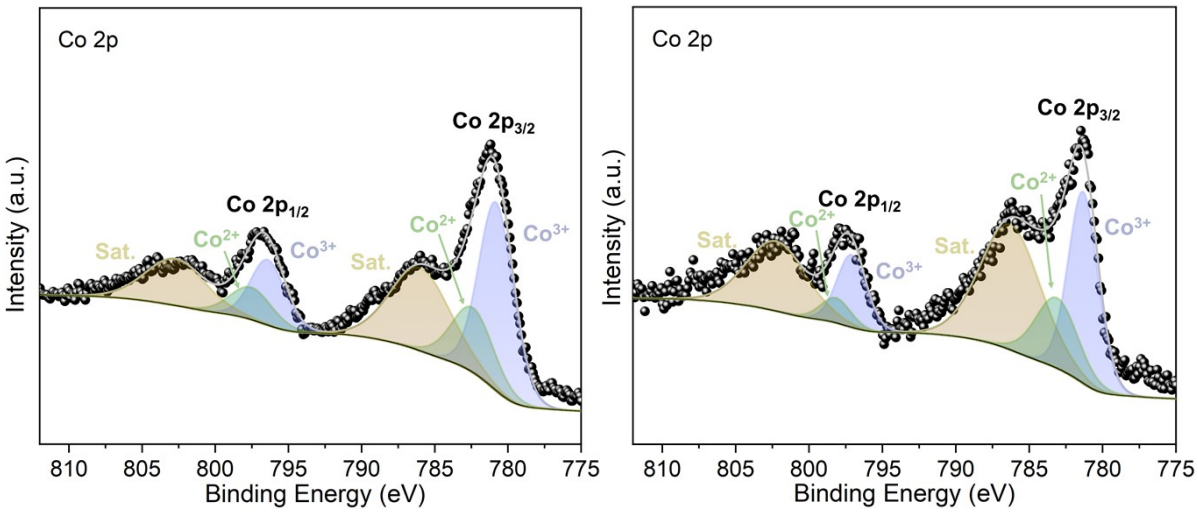

Figure S14. High-resolution Co 2p XPS spectra of Co@MOFs (left) and Co@Pt-SACs (right).

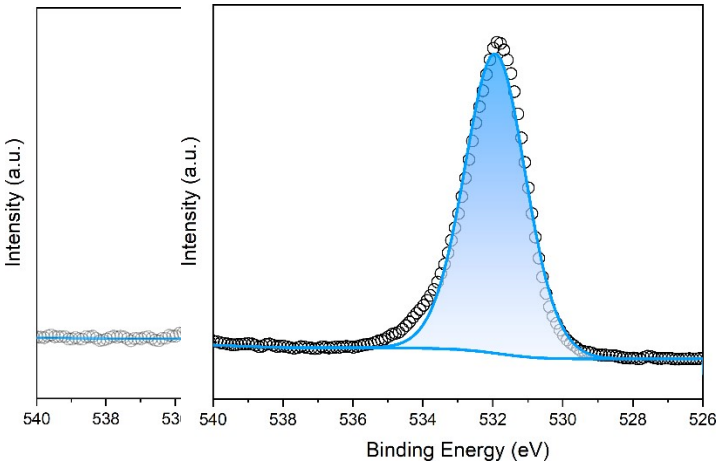

Figure S15. High-resolution O 1s XPS spectra of Co@MOFs (left) and Co@Pt-SACs (right).

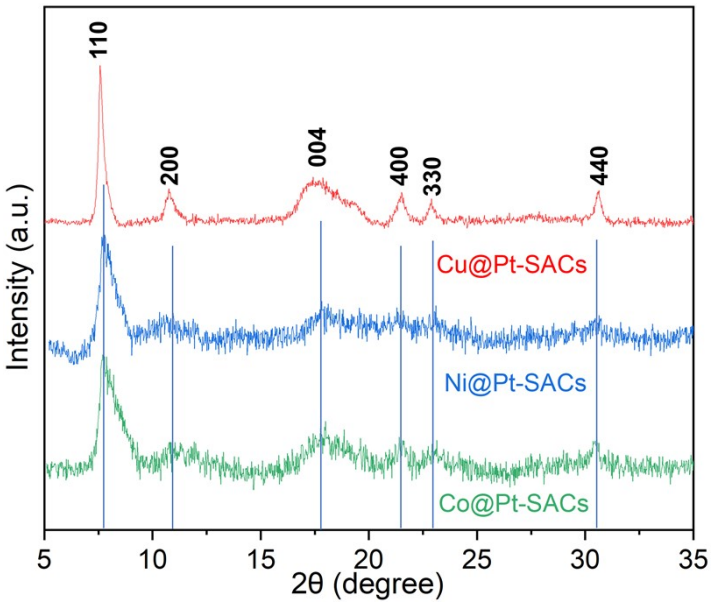

Figure S16. PXRD pattern of Cu@Pt-SACs, Ni@Pt-SACs and Co@Pt-SACs.

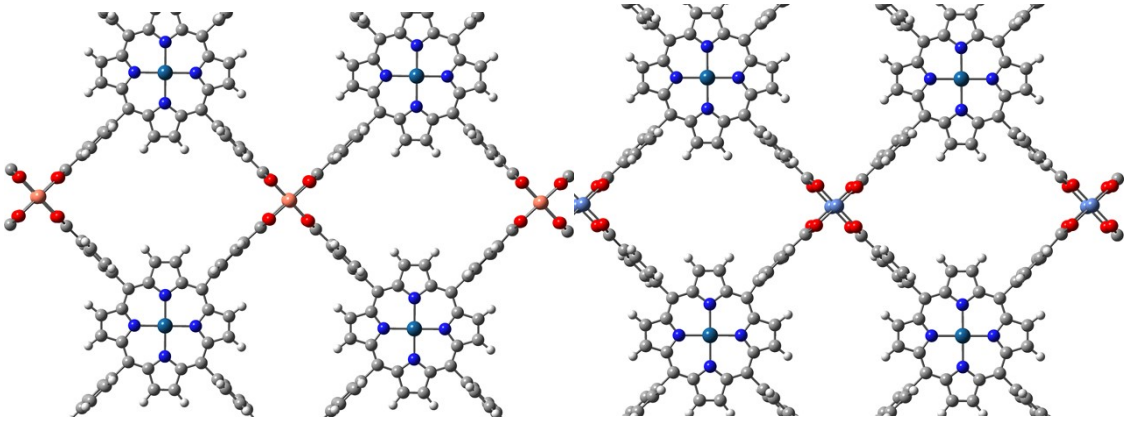

Figure S17. Single-atom catalysts Cu@Pt-SACs (left) and Ni@Pt-SACs (right) calculated by DFT simulations.

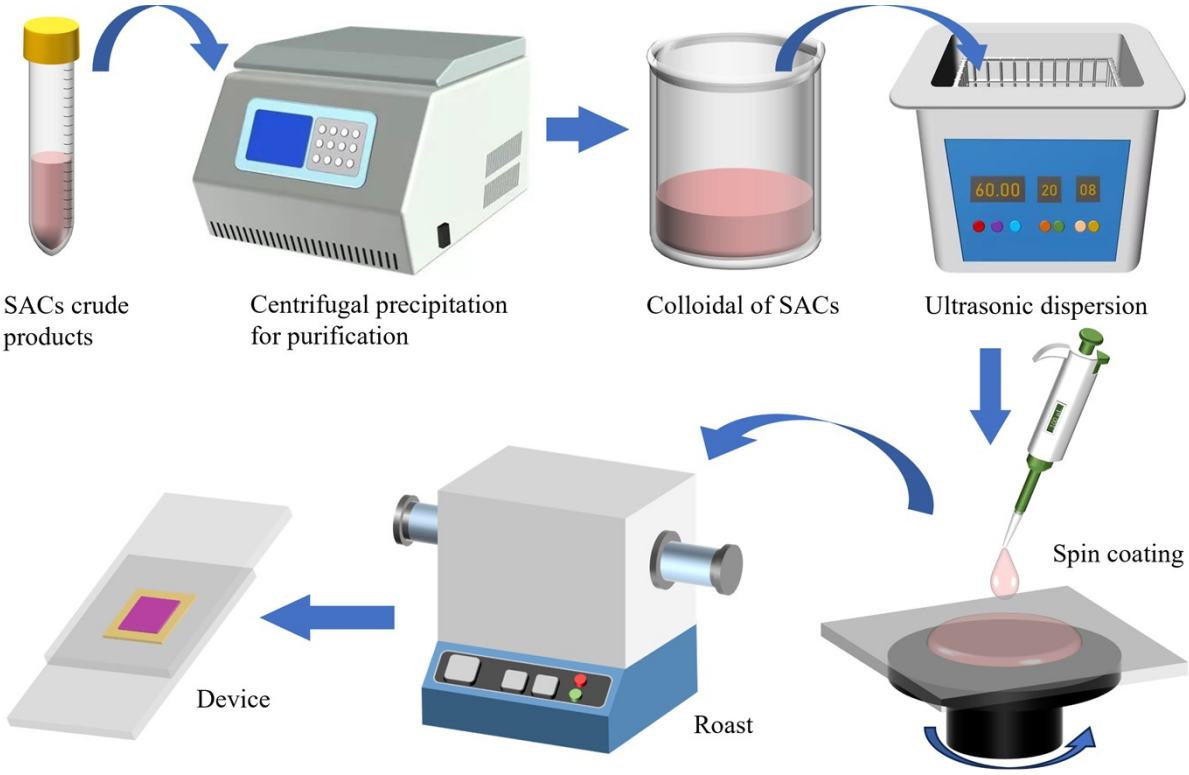

Figure S18. Schematic Illustration of Device Fabrication Using Single-Atom Catalysts (SACs). The ethanol colloid of Pt@SACs (1 g/mL) was centrifuged at 4000 rpm. Subsequently, the sample was subjected to ultrasonic dispersion for 5 minutes. The Pt@SACs ethanol colloid was then spin-coated onto the surface of a Pt electrode at 3000 rpm. Following this, nitrogen was introduced into the tube furnace, and the electrode was sintered at 300°C for 15 minutes to obtain the Pt@SACs electrode.

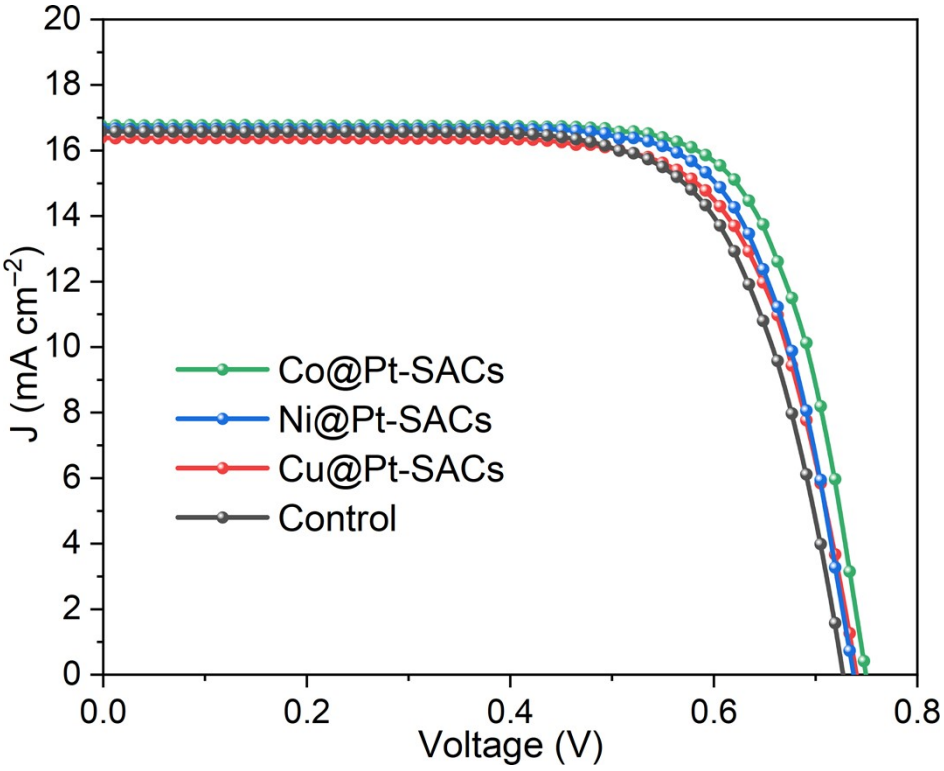

Figure S19. *J*−*V* curves under reverse scan and the champion PCE of different DSSCs.

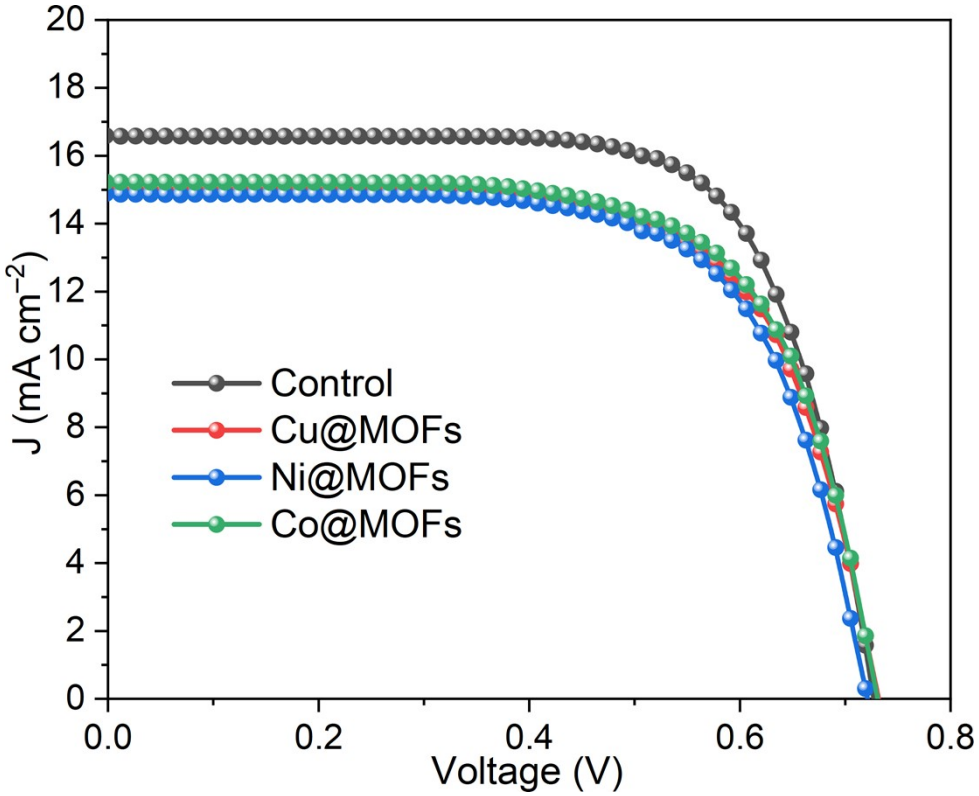

Figure S20. *J*−*V* curves under reverse scan and the champion PCE of different DSSCs.

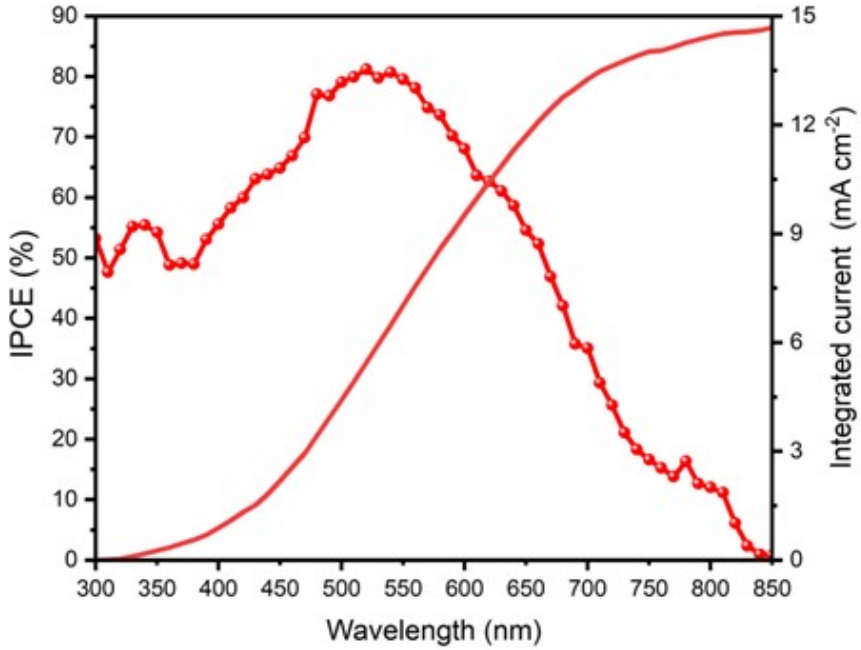

Figure S21. IPCE curve and integral current for Co@Pt-SACs device.

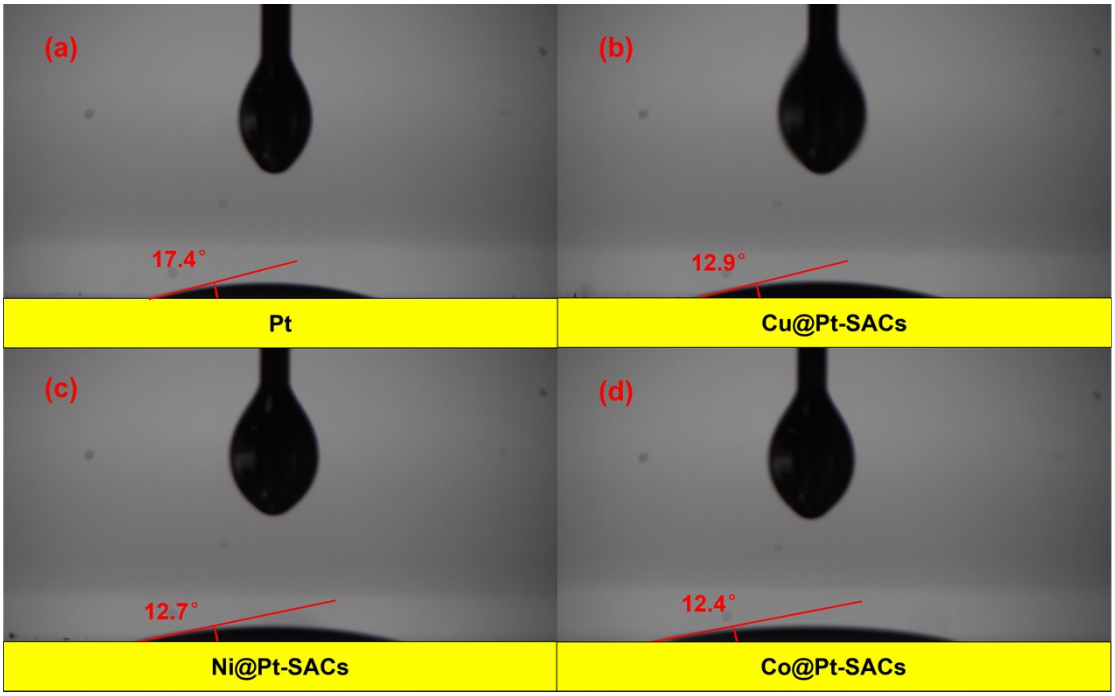

Figure S22. Contact angle tests were performed using Pt, Cu@Pt-SACs, Ni@Pt-SACs and Co@Pt-SACs as counter electrodes.

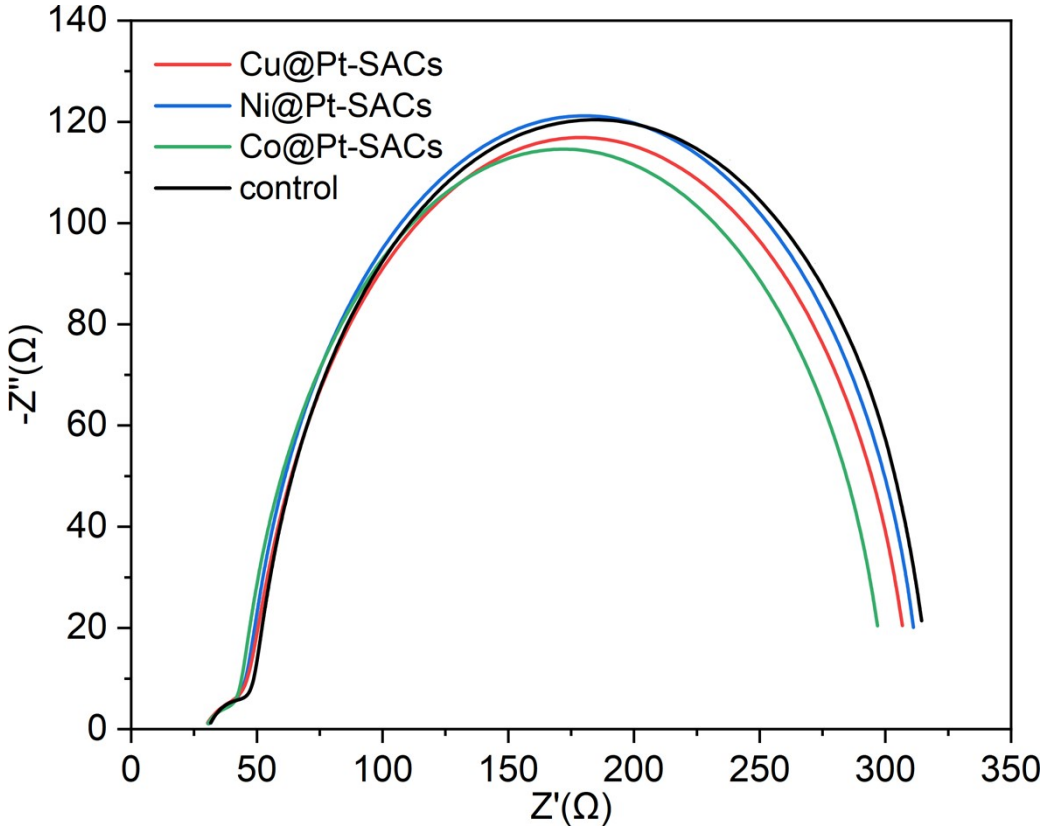

Figure S23. Electrochemical impedance spectroscopy (EIS) Nyquist plots of different CE and the matching equivalent-circuit diagram.

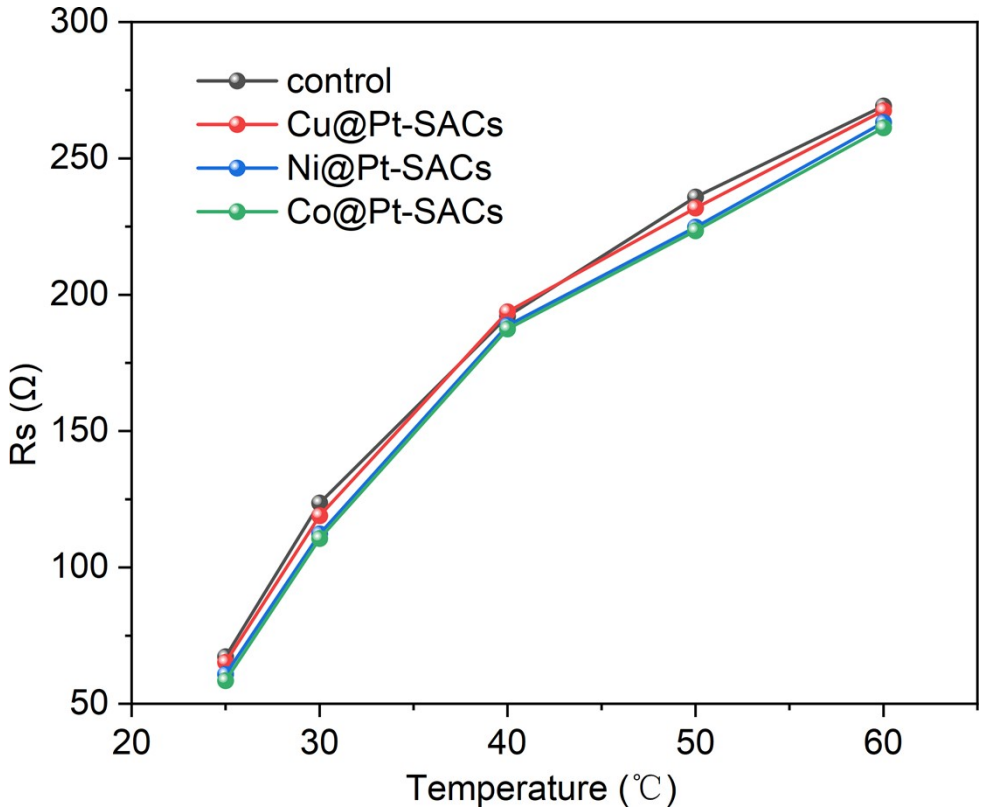

Figure S24. Impedance testing of four devices at different temperatures.

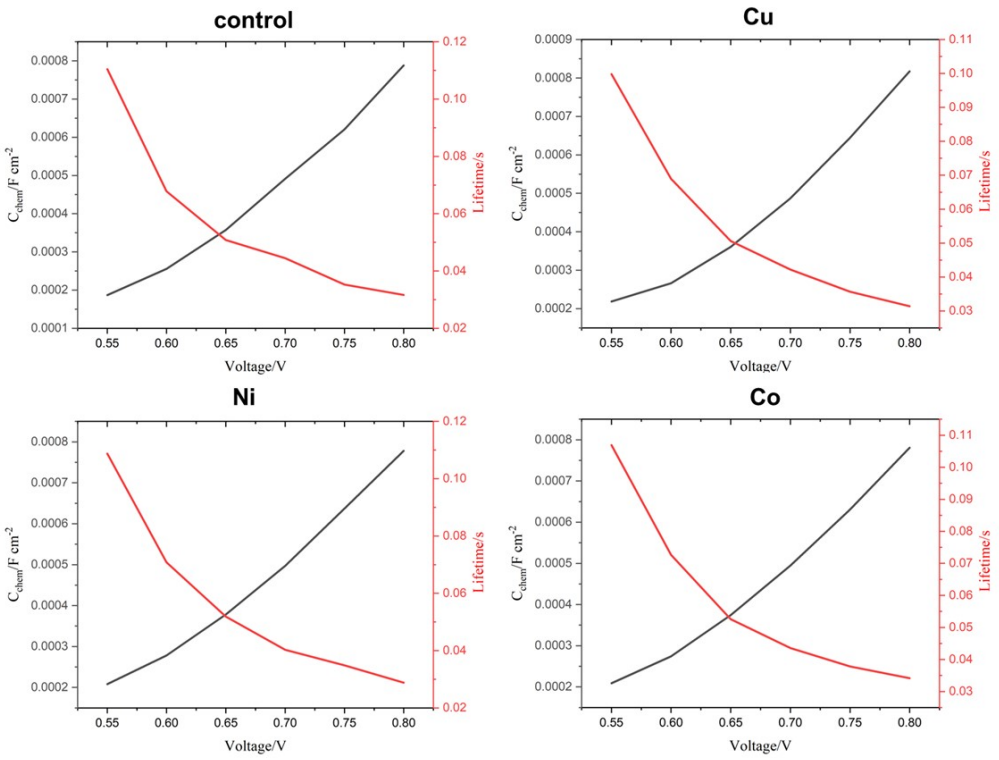

Figure S25. Capacitance and electronic life testing of four devices.

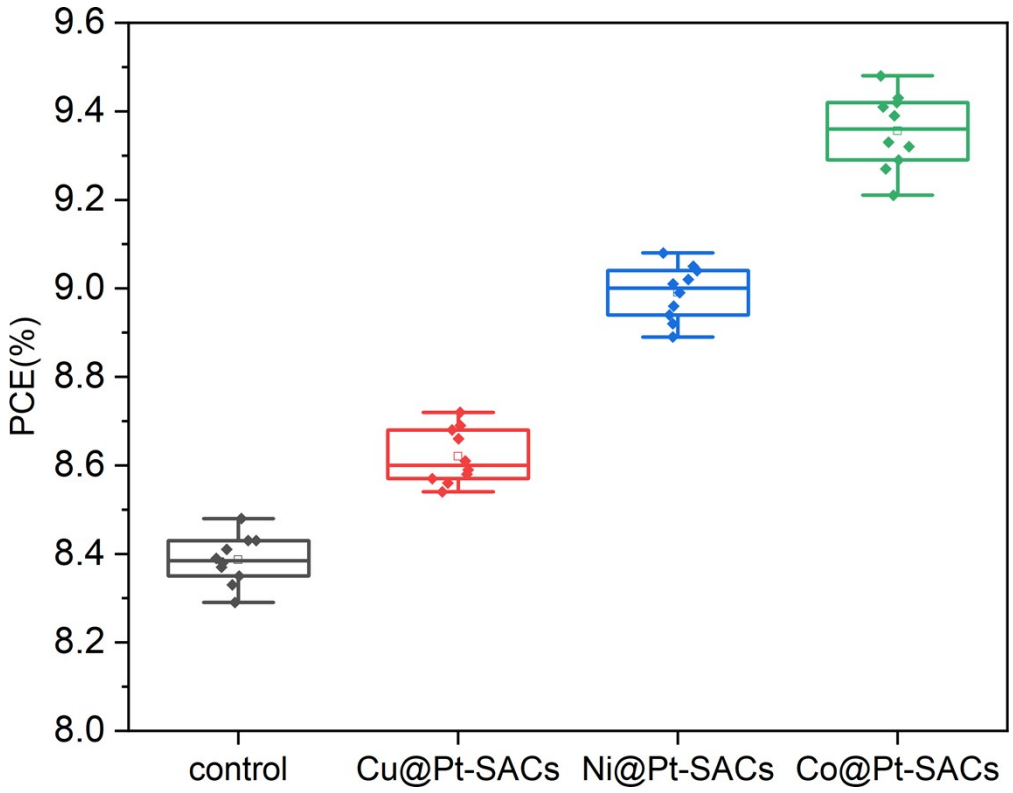

Figure S26. Ten box plots of each of the four devices were prepared for equilibrium testing.

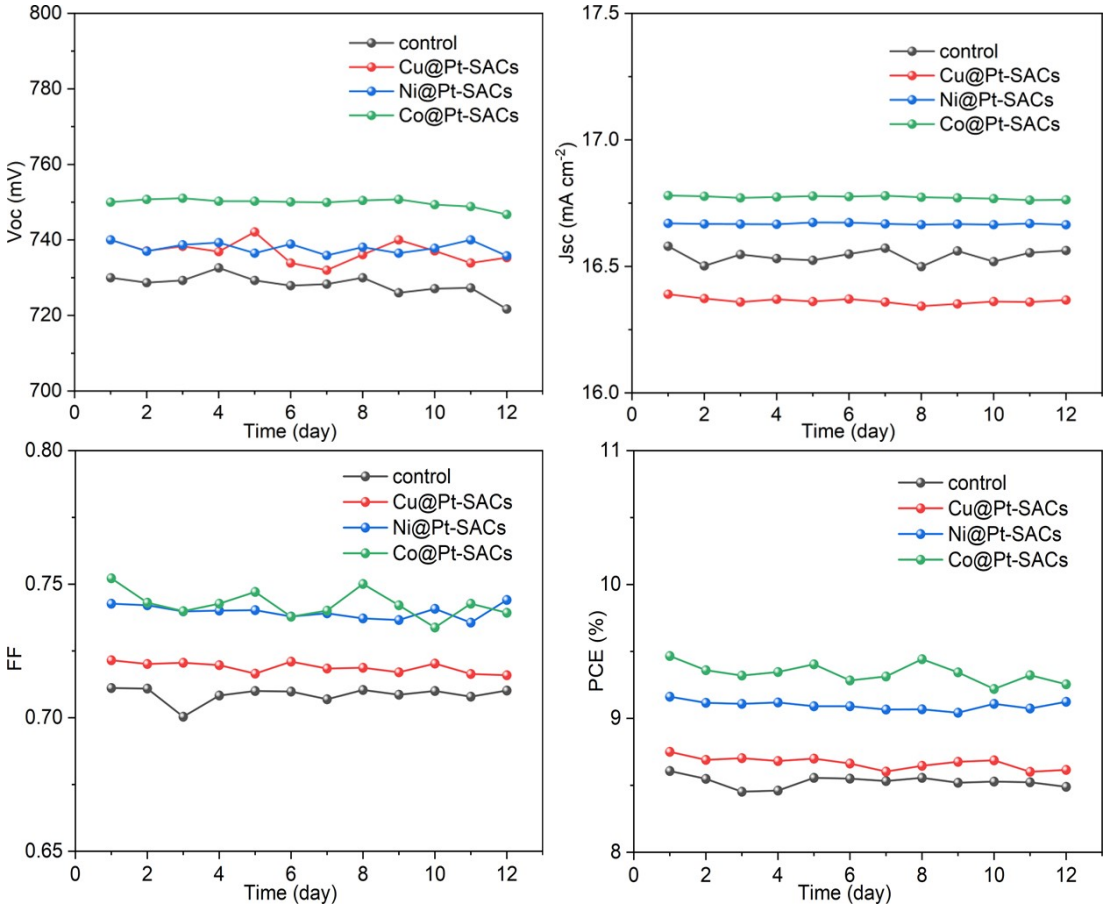

Figure S27. Stability test based on four devices at 50°C with continuous light.

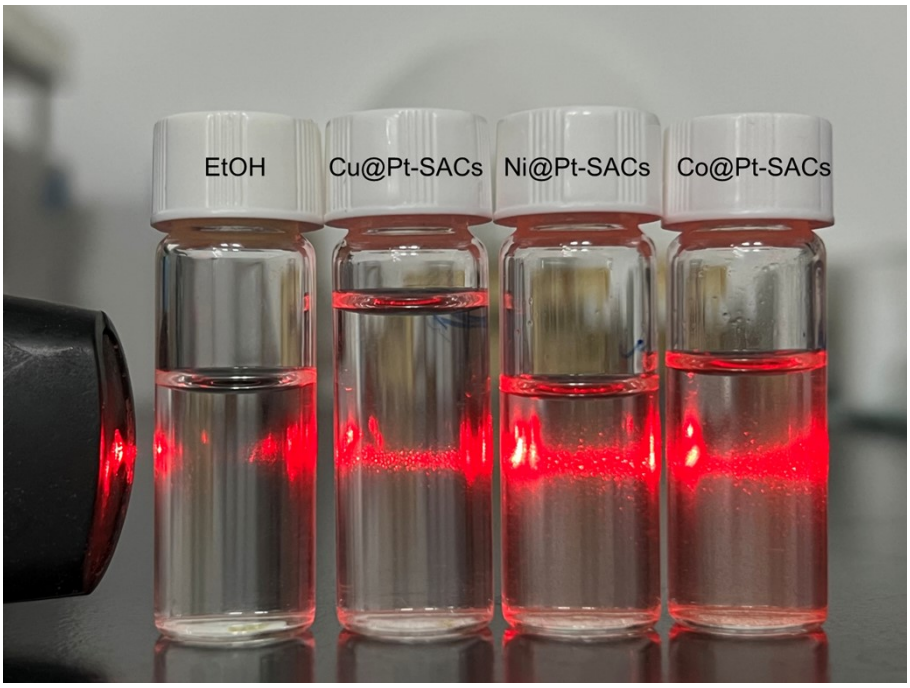

Figure S28. The newly synthesized Pt@SACs (from left to right: ethanol, Cu@Pt-SACs, Ni@Pt-SACs, and Co@Pt-SACs) can be redispersed in ethanol to form a colloidal suspension. Laser irradiation produces the Tyndall effect.

Table S1. The actual Pt contents in the catalysts evaluated by ICP-OES and XPS analyses

samples	Cu@Pt-SACs	Ni@Pt-SACs	Co@Pt-SACs
Pt (wt%)	11.74	11.69	11.87

Table S2. *J*−*V* curves under reverse scan and the champion PCE of different DSCs.

CE	V_{oc}/V	J_{sc}/mA cm^{-2}	*FF*	PCE (%)
Co@Pt-SACs	0.75	16.78	75.22	9.46
Ni@Pt-SACs	0.74	16.67	74.27	9.13
Cu@Pt-SACs	0.74	16.39	72.15	8.75
Pt	0.73	16.58	71.11	8.57

Table S3. Performance comparison of this work and the reported different single-atom counter electrode materials.

CE	V_{oc}/V	J_{sc}/mA cm^{-2}	*FF*	PCE (%)
Co@Pt-SACs	0.75	16.78	75.22	9.46
Ni@Pt-SACs	0.74	16.67	74.27	9.13
Cu@Pt-SACs	0.74	16.39	72.15	8.75
2S2-N-Co_1/C [S1]	0.82	12.75	75.86	7.98
S2-NCo_1/C [S1]	0.83	12.10	76.10	7.68
CoN_4/GN [S2]	0.72	17.32	67.36	8.40
NiN_4/GN [S2]	0.71	17.93	59.91	7.62
CuN_4/GN [S2]	0.70	15.95	57.77	6.45
Mo/Co-N-C [S3]	0.75	15.65	0.69	7.98
Bi/Co-N-C [S3]	0.78	14.92	0.66	7.65
Nb/Co-N-C [S3]	0.75	15.14	0.66	7.46
Ti_1/NC-SAC [S4]	0.78	16.71	0.63	8.21
Ni-SAC [S5]	0.72	15.50	0.67	7.42

Table S4. *J*−*V* curves under reverse scan and the champion PCE of different DSCs.

CE	V_{oc}/V	J_{sc}/mA cm^{-2}	*FF*	PCE (%)
Pt	0.73	16.58	71.11	8.57
Cu@MOFs	0.73	14.97	67.65	7.41
Ni@MOFs	0.72	14.87	67.62	7.25
Co@MOFs	0.73	15.22	67.81	7.54

Table S5. The photoelectric parameters of single DSSCs (Pt, Cu@Pt-SACs, Ni@Pt-SACs and Co@Pt-SACs)

CE	R_s /Ω	R_{ct} /Ω	Z_N /Ω
Pt	31.59	11.50	271.32
Cu@Pt-SACs	30.40	10.88	265.44
Ni@Pt-SACs	30.81	10.77	269.60
Co@Pt-SACs	30.46	10.46	256.45

Table S6. Impedance testing of device (Pt, Cu@Pt-SACs, Ni@Pt-SACs and Co@Pt-SACs) at different temperatures.

Temperature (℃)	Pt	Cu@Pt-SACs	Ni@Pt-SACs	Co@Pt-SACs
25	67.23	65.18	60.86	58.52
30	123.65	118.97	112.31	110.61
40	192.12	193.75	188.72	187.44
50	235.85	231.81	224.79	223.45
60	269.23	267.53	263.21	261.21

Table S7**.** EXAFS data fitting parameters and results for Co@Pt-SACs

Samples	Path	Bond length	δ^2 (10^{-3}Å^2)	Coordination number
Co@Pt-SACs	Pt-N	2.05	6.3	3.7

Error bounds (accuracies) were estimated as Coordination Number, ±5%; Bond length, ±1%; δ^2 (Debye-Waller factor), ±5%.

REFERENCES

[S1] Jing, H.; Zhao, Z.; Zhang, C.; Liu, W.; Wu, D.; Zhu, C.; Hao, C.; Zhang, J.; Shi, Y., Tuned single atom coordination structures mediated by polarization force and sulfur anions for photovoltaics. *Nano Res.* **2021**, *14*, 4025-4032.

[S2] Cui, X.; Xiao, J.; Wu, Y.; Du, P.; Si, R.; Yang, H.; Tian, H.; Li, J.; Zhang, W.; Deng, D.; Bao, X., A Graphene Composite Material with Single Cobalt Active Sites: A Highly Efficient Counter Electrode for Dye-Sensitized Solar Cells. *Angew. Chem. Int. Ed.* **2016**, *55*, 6708-6712.

[S3] Zafar, N.; Yun, S.; Sun, M.; Shi, J.; Arshad, A.; Zhang, Y.; Wu, Z. Cobalt-Based Incorporated Metals in Metal−Organic Framework-Derived Nitrogen-Doped Carbon as a Robust Catalyst for Tri-iodide Reduction in Photovoltaics. ACS Catal. 2021, 11, 13680-13695.

[S4] Xin, C.; Liang, S.; Hu, J.; Guo, J.; Cheng, X.; Shang, W.; Wei, J.; Zhang, S.; Liu, W.; Zhu, C.; Hou, j.; Shi, Y. In-Situ Grafting of Single-Atomic Titanium–Nitrogen Moiety onto Carbon Nanostructures for Efficient Photovoltaic Devices. ACS Appl. Mater. Interfaces. 2022, 14(45): 50849-50857.

[S5] Lin, D.; Jiang, R.; Ma, P.; Hong, S.; Cheng, Z.; Guo, J.; Xu, R.; Li, Y.; Zhao, Y.; Yin, X.; Wang, L. Nickel-Based Single-Atom Catalyst toward Triiodide Reduction Reaction in Hybrid Photovoltaics. ACS Sustainable Chem. Eng. 2021, 9, 4256-4261.